Semiannual Technical Report

Atomic Layer Epitaxy of Group IV Materials: Surface Processes, Thin Films, Devices and Their Characterization

Supported under Grant #N00014-91-J-1416
Office of the Chief of Naval Research
Report for the period 1/1/96–6/30/96

R. F. Davis, S. Bedair*, N. A. El-Masry, Z. Sitar,
S. K. Han, R. Leonard, S. Liu, M. T. McClure,
F. G. McIntosh, and A. H. Morshed*
c/o Materials Science and Engineering Department
and *Electrical and Computer Engineering Department
North Carolina State University
Campus Box 7907
Raleigh, NC 27695-7907

June, 1996

DISCLAIMER NOTICE

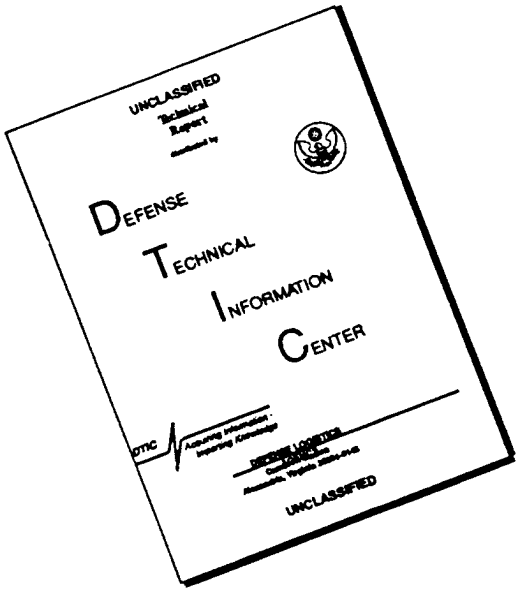

THIS DOCUMENT IS BEST QUALITY AVAILABLE. THE COPY FURNISHED TO DTIC CONTAINED A SIGNIFICANT NUMBER OF PAGES WHICH DO NOT REPRODUCE LEGIBLY.

REPORT DOCUMENTATION PAGE

Form Approved
OMB No. 0704-0188

1. AGENCY USE ONLY *(Leave blank)*	2. REPORT DATE	3. REPORT TYPE AND DATES COVERED
	June, 1996	Semiannual Technical 1/1/96–6/30/96

4. TITLE AND SUBTITLE
Atomic Layer Epitaxy of Group IV Materials: Surface Processes, Thin Films, Devices and Their Characterization

5. FUNDING NUMBERS
414v001---01
1114SS
N00179
N66005
4B855

6. AUTHOR(S)
Robert F. Davis

7. PERFORMING ORGANIZATION NAME(S) AND ADDRESS(ES)
North Carolina State University
Hillsborough Street
Raleigh, NC 27695

8. PERFORMING ORGANIZATION REPORT NUMBER
N00014-91-J-1416

9. SPONSORING/MONITORING AGENCY NAMES(S) AND ADDRESS(ES)
Sponsoring: ONR, Code 312, 800 N. Quincy, Arlington, VA 22217-5660
Monitoring: Administrative Contracting Officer, ONR, Regional Office Atlanta
101 Marietta Tower, Suite 2805
101 Marietta Street
Atlanta, GA 30323-0008

10. SPONSORING/MONITORING AGENCY REPORT NUMBER

11. SUPPLEMENTARY NOTES

12a. DISTRIBUTION/AVAILABILITY STATEMENT
Approved for Public Release; Distribution Unlimited

12b. DISTRIBUTION CODE

13. ABSTRACT *(Maximum 200 words)*

The growth parameter, α, the ratio of the growth rates on {100} and {111} facets for diamond films deposited on Si and Ti by microwave plasma CVD has been studied using SEM micrographs. Different morphologies were generated on Si under different deposition conditions. The value of α increased with decreasing temperature and increasing methane concentration, as expected. A value of α for Ti was not obtained due to the heavily twinned particles. Violet/blue photoluminescence from epitaxial cerium dioxide films on Si substrates was observed for the first time. The films were deposited on Si(111) substrates under UHV conditions using pulsed laser ablation of a cerium oxide target. They were rapid thermally annealed in argon, and excited by a He-Cd ultraviolet laser of 325 nm wavelength. The emission might be due to charge transfer transitions from the 4f band to the valence band of CeO_2. Growth of Si on nearly lattice matched CeO_2/Si(111) substrates for silicon-on-insulator (SOI) applications is reported. A low pressure chemical vapor deposition (LPCVD) growth technique was employed using 1% disilane in N_2 to deposit silicon at 700 and 750°C on single crystal CeO_2 films deposited under UHV conditions in the same growth apparatus. The RHEED patterns obtained and the surface morphology of the grown films indicated a three-dimensional mode of crystal growth.

14. SUBJECT TERMS
diamond, films, silicon, titanium, growth parameter, morphology, twinning, cerium dioxide, photoluminescence, Si(111), pulsed laser ablation, silicon-on-insulator, low pressure chemical vapor deposition, RHEED

15. NUMBER OF PAGES
21

16. PRICE CODE

17. SECURITY CLASSIFICATION OF REPORT	18. SECURITY CLASSIFICATION OF THIS PAGE	19. SECURITY CLASSIFICATION OF ABSTRACT	20. LIMITATION OF ABSTRACT
UNCLAS	UNCLAS	UNCLAS	SAR

Table of Contents

I.	Introduction	1
II.	Influence of Temperature and Methane Concentration on the Diamond Growth Parameter α on Silicon and Titanium Substrates	3
III.	Optical Properties of Epitaxial CeO_2 on Silicon Substrates	11
IV.	Deposition of Crystalline Silicon on Lattice Matched CeO_2/Si(111) Substrates	18
V.	Distribution List	21

I. Introduction

Atomic layer epitaxy (ALE) is the sequential chemisorption of one or more elemental species or complexes within a time period or chemical environment in which only one monolayer of each species is chemisorbed on the surface of the growing film in each period of the sequence. The excess of a given reactant which is in the gas phase or only physisorbed is purged from the substrate surface region before this surface is exposed to a subsequent reactant. This latter reactant chemisorbs and undergoes reaction with the first reactant on the substrate surface resulting in the formation of a solid film. There are essentially two types of ALE which, for convenience, shall be called Type I and Type II.

In its early development in Finland, the Type I growth scenario frequently involved the deposition of more than one monolayer of the given species. However, at that time, ALE was considered possible only in those materials wherein the bond energies between like metal species and like nonmetal species were each less than that of the metal-nonmetal combination. Thus, even if multiple monolayers of a given element were produced, the material in excess of one monolayer could be sublimed by increasing the temperature and/or waiting for a sufficient period of time under vacuum. Under these chemical constraints, materials such as GaAs were initially thought to be improbable since the Ga-Ga bond strength exceeds that of the GaAs bond strength. However, the self-limiting layer-by-layer deposition of this material proved to be an early example of Type II ALE wherein the trimethylgallium (TMG) chemisorbed to the growing surface and effectively prevented additional adsorption of the incoming metalorganic molecules. The introduction of As, however caused an exchange with the chemisorbed TMG such that a gaseous side product was removed from the growing surface. Two alternating molecular species are also frequently used such that chemisorption of each species occurs sequentially and is accompanied by extraction, abstraction and exchange reactions to produce self-limiting layer-by-layer growth of an element, solid solution or a compound.

The Type II approach has been used primarily for growth of II–VI compounds [1–13]; however, recent studies have shown that it is also applicable for oxides [14–17], nitrides [18], III–V GaAs-based semiconductors [19–32] and silicon [33–35]. The advantages of ALE include monolayer thickness control, growth of abrupt interfaces, growth of uniform and graded solid solutions with controlled composition, reduction in macroscopic defects and uniform coverage over large areas. A commercial application which makes use of the last attribute is large area electroluminescent displays produced from II–VI materials. Two comprehensive reviews [36,6], one limited overview [37] and a book [38] devoted entirely to the subject of ALE have been published.

In this reporting period, investigations concerned with (1) the determination of the growth parameter, α, for diamond films on Si and Ti, (2) the deposition, annealing and determination of the optical emission of CeO_2 epitaxial films on Si(100), and (3) the growth of Si on nearly

lattice matched CeO_2/Si(111) substrates for silicon-on-insulator (SOI) applications have been conducted.

The following sections introduce each topic, detail the experimental approaches, report the results to date and provide a discussion and a conclusion for each material. Each major section is self-contained with its own figures, tables and references.

References

1. T. Suntola and J. Antson, U.S. Patent 4,058,430, 1977.
2. M. Ahonen, M. Pessa and T. Suntola, Thin Solid Films **65**, 301, 1980.
3. M. Pessa, R. Makela, and T. Suntola, Appl. Phys. Lett. **38**, 131, 1981.
4. T. Yao and T. Takeda, Appl. Phys. Lett. **48**, 160, 1986.
5. T. Yao, T. Takeda, and T. Watanuki, Appl. Phys. Lett. **48**, 1615, 1986.
6. T. Yao, Jpn. J. Appl. Phys. **25**, L544, 1986.
7. T. Yao and T. Takeda, J. Cryst. Growth **81**, 43, 1987.
8. M. Pessa, P. Huttunen and M. A. Herman, J. Appl. Phys. **54**, 6047, 1983.
9. C. H. L. Goodman and M. V. Pessa, J. Appl. Phys. **60**, R65, 1986.
10. M. A. Herman, M. Valli and M. Pessa, J. Cryst. Growth **73**, 403, 1985.
11. V. P. Tanninen, M. Oikkonen and T. Tuomi, Phys. Status Solidi **A67**, 573, 1981.
12. V. P. Tanninen, M. Oikkonen and T. Tuomi, Thin Solid Films **90**, 283, 1983.
13. D. Theis, H. Oppolzer, G. Etchinghaus and S. Schild, J. Cryst. Growth **63**, 47, 1983.
14. S. Lin, J. Electrochm. Soc. **122**, 1405, 1975.
15. H. Antson, M. Leskela, L. Niinisto, E. Nykanen and M. Tammenmaa, Kem.-Kemi **12**, 11, 1985.
16. R. Tornqvist, Ref. 57 in the bibliography of Chapt. 1 of Ref. 38 of this report.
17. M. Ylilammi, M. Sc. Thesis, Helsinki Univ. of Technology, Espoo, 1979.
18. I. Suni, Ref. 66 in the bibliography of Chapt. 1 of Ref. 38 in this report.
19. S. M. Bedair, M. A. Tischler, T. Katsuyama and N. A. El-Masry, Appl. Phys. Lett. **47**, 51, 1985.
20. M. A. Tischler and S. M. Bedair **48**, 1681, 1986.
21. M. A. Tischler and S. M. Bedair, J. Cryst. Growth **77**, 89, 1986.
22. M. A. Tischler, N. G. Anderson and S. M. Bedair, Appl. Phys. Lett. **49**, 1199, 1986.
23. M. A. Tischler, N. G. Anderson, R. M. Kolbas and S. M. Bedair, Appl. Phys. Lett. **50**, 1266, 1987.
24. B. T. McDermott, N. A. El-Masry, M. A. Tischler and S. M. Bedair, Appl. Phys. Lett. **51**, 1830, 1987.
25. M. A. Tischler, N. G. Anderson, R. M. Kolbas and S. M. Bedair, SPIE Growth Comp. Semicond. **796**, 170, 1987.
26. S. M. Bedair in Compound Semiconductor Growth Processing and Devices for the 1990's, Gainesville, FL, 137, 1987.
27. J. Nishizawa, H. Abe and T. Kurabayashi, J. Electrochem. Soc. **132**, 1197, 1985.
28. M. Nishizawa, T. Kurabayashi, H. Abe, N. Sakurai, J. Electrochm. Soc. **134**, 945, 1987.
29. P. D. Dapkus in Ref. 27, in the bibliography of Chapt. 1 of Ref. 38 in this report.
30. S. P. Denbaars, C. A. Beyler, A. Hariz, P. D. Dapkus, Appl. Phys. Lett. **51**, 1530, 1987.
31. M. Razeghi, Ph. Maurel, F. Omnes and J. Nagle, Appl. Phys. Lett. **51**, 2216, 1987.
32. M. Ozeki, K. Mochizuki, N. Ohtsuka, K. Kodama, J. Vac. Sci. Technol. **B5**, 1184, 1987.
33. Y. Suda, D. Lubben, T. Motooka and J. Greene, J. Vac. Sci. Technol. **B7**, 1171, 1989.
34. J. Nishizawa, K. Aoki, S. Suzuki and K. Kikuchi, J. Cryst. Growth **99**, 502, 1990.
35. T. Tanaka, T. Fukuda, Y. Nagasawa, S. Miyazaki and M. Hirose, Appl. Phys. Lett. **56**, 1445, 1990.
36. T. Suntola and J. Hyvarinen, Ann. Rev. Mater. Sci. **25**, 177, 1985.
37. M. Simpson and P. Smith, Chem. Brit. **23**, 37, 1987.
38. T. Suntola and M. Simpson, *Atomic Layer Epitaxy*, Chapman and Hall, New York, 1990.

II. Influence of Temperature and Methane Concentration on the Diamond Growth Parameter α on Silicon and Titanium Substrates

A. Introduction

Diamond has become an enticing candidate for high-power, high-frequency electronic device applications in high-temperature or chemically-harsh environments. However, to realize its true potential, single-crystal diamond films are needed. Although economically viable sizes and quantities of substrates for single-crystal diamond films are still not available, there has been significant progress on oriented diamond films [1-3]. Under certain growth conditions, strongly oriented diamond films can be obtained by taking advantage of the growth competition between differently oriented diamond grains [4]. In order to take advantage of the texture evolution process, it is essential to understand the growth parameter α which is given by the relative growth rates on {100} and {111} facets [5-7]. The growth parameter α can be represented by the simple formula, $\alpha = \sqrt{3}\,(V_{100}/V_{111})$ where V_{100} and V_{111} are the growth rates on the {100} and {111} faces, respectively.

To gain the precise information about the growth parameter α on silicon and titanium in our system, investigation of the dependence of the morphology of diamond films on methane concentration and deposition temperature was undertaken. After deposition, the morphology of each sample was examined by the scanning electron microscope (SEM). The values of α were determined by comparing the surface morphologies with the idiomorphic crystal shapes for different values of α described by Wild [6]. While there have been some experimental results of the growth parameter α on silicon, understanding the growth parameter α on titanium remains elusive. Investigating the α parameter space on titanium is desirable because of its potential application as an interlayer for diamond nucleation on otherwise "difficult to nucleate" materials, such as copper and steel. Also, comparison of "α maps" for silicon and titanium may elucidate some mechanisms of diamond growth.

B. Experimental Procedure

Substrate Preparation. The polycrystalline titanium samples were polished using progressively finer media. The polishing scheme started with 600 grit SiC, then 30μm and 6μm diamond powder and finished using a colloidal silica solution that polished by mechanical and chemical means. Following the polishing, the sample was cleaned by acetone, methanol, and isopropanol. The silicon (100) substrates were etched in dilute HF acid prior to insertion into the chamber.

Four-step Deposition Process. The four-step deposition process consisted of a hydrogen plasma clean, surface carburization, biased enhanced nucleation (BEN), and growth. Hydrogen plasma clean was performed for 30 minutes to remove any carbonaceous residue on

the substrates. Following the hydrogen plasma clean, the carburization step was undertaken for 30 minutes at 2% methane/hydrogen concentration at 25 Torr. After the carburization step, the samples were subjected to a nucleation step. At the nucleation step, the chamber pressure was reduced to 20 Torr and methane/hydrogen ratio was increased to 5%. Then a negative DC voltage, about -240 V, was applied to the substrate for 8 minutes. At the end of the biasing step, the bias voltage was terminated and the pressure was raised to 25 Torr. In the growth stage, the substrate position and methane/hydrogen concentration was changed to the desired point. Table I summarizes the system parameters for each step.

Table I. Summary of System Parameters

Parameters	H_2 Plasma Clean	Carburization	BEN	Growth
Power	600W	600W	600W	600W
Pressure	25 Torr	25 Torr	20 Torr	25 Torr
CH_4/H_2 ratio	-	2%	5%	varied
Bias Current	-	-	80 mA	-
Bias Voltage	-	-	-240V	-
Temperature	700°C	800°C	850°C	varied
Duration	30 minutes	30 minutes	8 minutes	16-17 hours

Growth Conditions. From previous experience, the following upper and lower limits on methane concentration (0.1%–1.0%) and deposition temperature (700°C–900°C) were chosen. In order to have the best representative data points, a statistical experimental design software package (Strategy) was used to determine the different deposition conditions within the limits. The resulting deposition was observed by SEM and isolated diamond particles were examined to determine the α value. Approximate α values were assigned using the idiomorphic crystal shapes described by Wild [6] and further discussed by Tamor [7]. Although a different chamber system and operating parameters were used, the diagram composed by both researchers gave a general gradient of α. The idiomorphic crystal shapes and α diagram composed by Wild is in Fig. 1. The value of α increased with decreasing deposition temperature and increasing methane concentration. Table II summarizes the five different deposition conditions.

C. Results and Discussion

Deposition on Silicon. Well-defined facets were observed at all deposition conditions, except for the low methane concentration and low temperature sample (Sample 4). The

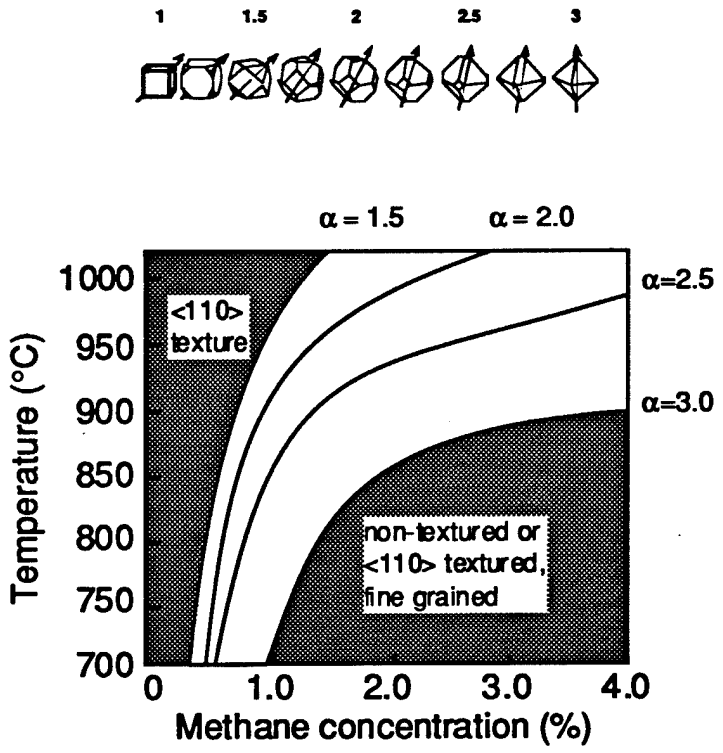

Figure 1. Idiomorphic crystal shapes and α diagram composed by Wild.

Table II. Deposition Conditions for Each Sample

Sample Number	CH_4%	Temperature
1	0.27	900±10
2	1.00	700±10
3	0.60	800±10
4	0.10	700±10
5	0.93	900±10

corresponding α value and SEM image of each sample is shown in Table III and Figs. 2(a-d), respectively. The diamond crystals on the Sample 1 showed cubo-octahedral shape morphology as in Fig. 2(a). Since adjacent (111) faces and adjacent (100) faces were touching, the corresponding α value was about 1.5. Figure 2(b) shows the crystal morphology of Sample 2 which had truncated-octahedral shaped crystals. Compared to the idiomorphic crystal shape for $\alpha = 2$, Sample 2 had slightly larger (100) faces. Thus, the α value for Sample 2 was determined to be about 2.2. Sample 3 had a similar particle morphology to Sample 2 (Figs. 2c and 2b, respectively), although the (100) faces appeared to cover more of the crystal surface

than in Sample 2. Therefore, the α value for Sample 3 should lie between 2.2 and 1.5 and a value of 2.0 was assigned. Sample 5 had a similar morphology to Sample 1 (i.e. adjacent (111) and adjacent (100) faces intersected at a point), corresponding to α value of 1.5. As expected, the gradient of α followed the same trend as discussed by Wild [6] and Tamor [7]. Alpha increased with decreasing deposition temperature and increasing methane concentration. Based on this preliminary evaluation, an initial α diagram for diamond growth on silicon is shown in Fig. 3.

Table III. Corresponding α Values for Each Sample

Sample Number	α Value on Si	α Value on Ti
1	1.5±0.1	heavily twined particles
2	2.2±0.1	"
3	2.0±0.1	"
4	heavily twined particles	"
5	1.5±0.1	"

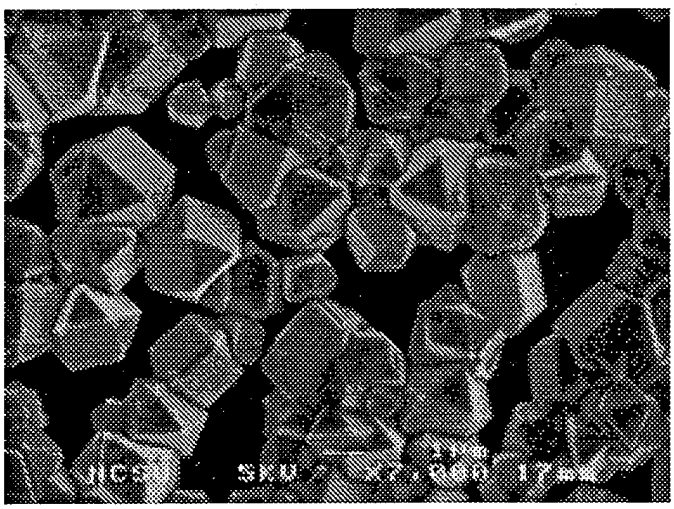

Figure 2(a). SEM image of Si Sample 1 ($CH_4\% = 0.27\%$, $T_{sub} = 900°C$).

(b)

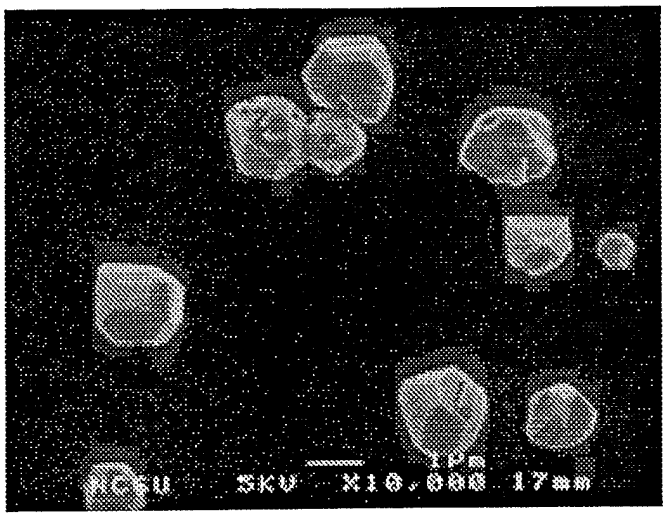

(c)

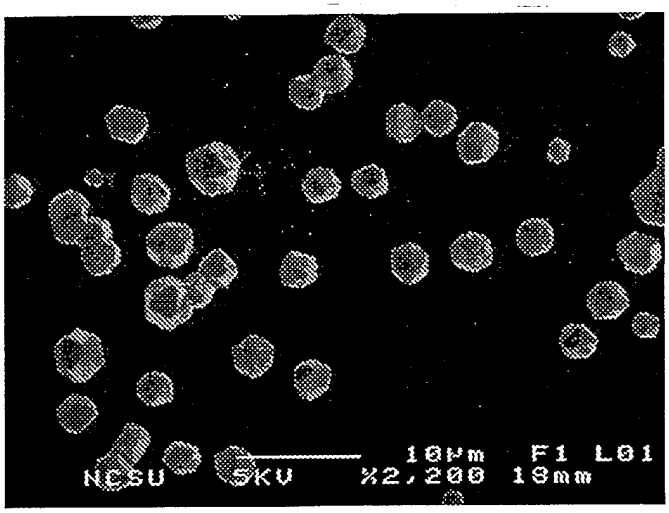

(d)

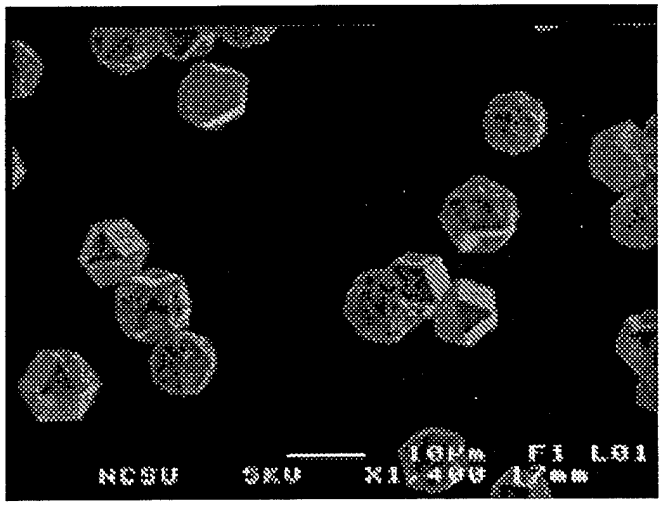

Figure 2 (b) SEM image of Si Sample 2 ($CH_4\% = 0.1\%$, $T_{sub} = 700°C$); (c) SEM image of Si Sample 3 ($CH_4\% = 0.6\%$, $T_{sub} = 800°C$); (d) SEM image of Si Sample 5 ($CH_4\% = 0.93\%$, $T_{sub} = 900°C$).

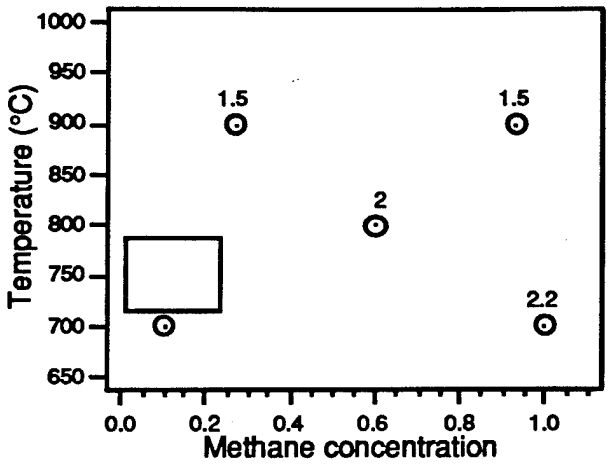

Figure 3. Alpha diagram for diamond growth on Si.

Deposition on Titanium. In the case of titanium, all of the samples had heavily twinned "cauliflower-like" morphologies as shown in Fig. 4. The absence of diamond particles with well-defined facets made determination of α impossible. In order to examine the growth parameter α on titanium, the twinning needed to be reduced as much as possible. There are several factors which may have contributed to the twinning of diamond on titanium: i) surface roughening after oxide removal, ii) hydride formation, iii) amorphous carbide formation, and iv) high surface mobility of carbon species. The first possible explanation for the twinning of diamond would be the surface roughening after oxide removal during the hydrogen plasma cleaning. Because titanium is a strong oxide former, substantial amount of oxide was likely formed during the substrate preparation stage. Since the interface between titanium and its oxide was probably not as smooth as the polished original surface, a rough surface would have resulted after etching by the hydrogen plasma. This rough surface may have contributed to the formation of twins in diamond. Another possible reason for heavy twinning can be found from its deposition environment. Throughout the deposition steps, titanium substrates were exposed to a hydrogen environment. Formation of a hydride could have occurred and would embrittle the titanium surface. As the substrate was heated by the plasma, differences in the thermal expansion coefficient may have caused cracking of the surface. These small cracks could have served as nucleating sites for non-uniform diamond particles and might have been responsible for heavily twined particles. The next factor may have been the formation of an amorphous carbide during the carburization step. Since amorphous carbide does not have long range order, it can easily contain defects that may contribute to the twinning. The last and more speculative reason would be the effect of surface mobility of carbon species on the titanium surface. Compared to silicon, titanium has much lower thermal conductivity; therefore, the surface temperature of titanium may have been higher than silicon. Since titanium might have had a

higher substrate temperature, the carbon species on titanium could migrate more easily, leading to a higher local carbon concentration. The higher carbon concentration would lead to twinning of the diamond crystals. Among the four factors, surface roughening after etching the titanium oxide layer, during the hydrogen plasma clean stage, is probably the most dominant factor, although further investigation is needed.

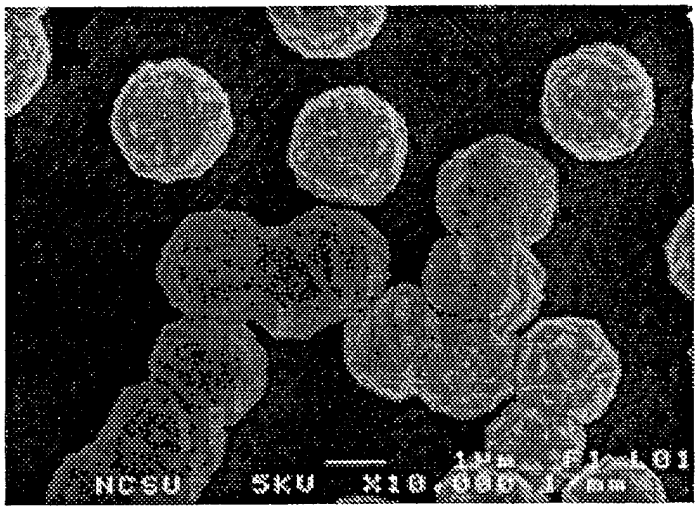

Figure 4. SEM image of typical diamond crystals on Ti.

D. Conclusions

The growth parameter α has been studied on silicon and titanium by investigating the dependence of films morphology on methane concentration and deposition temperature. On silicon, a range of α values was determined for diamond crystals deposited under a range of substrate temperature and methane concentration conditions. From this data, an initial α map was generated. The diagram confirmed the α gradient; the value of α increased with decreasing deposition temperature and increasing methane concentration. Under the same conditions, only heavily-twined diamond particles were found on the titanium substrates. Possible mechanisms which may have contributed to the twinning of diamond include surface roughening after oxide removal, hydride formation, amorphous carbide formation, and high surface mobility of carbon species. The surface roughening of the titanium after oxide etching is probably the most dominant factor.

E. Future Research Plans and Goals

In order to have a more detailed diagram, more samples with different methane concentrations and deposition temperatures need to be examined. The goal of this research is to grow highly oriented (100)-faceted diamond film on a silicon (100) substrate. On titanium substrate, since well-faceted diamond particles could not obtained, non-twined diamond

particles need to be nucleated in order to study the growth parameter α. To reduce the effects of surface oxide layer, it is planned to deposit a thin layer of titanium on silicon then transfer the sample to microwave plasma chemical vapor deposition system to grow diamond. Since the evaporation deposition system is connected to the microwave plasma chemical vapor deposition system, the sample can be transferred between two chambers without exposing it to air.

F. References

1. B. A. Fox, B. R. Stoner, D. M. Malta and P. J. Ellis, Diamond and Related Materials **3**, 382, 1994.
2. R. Beckman, W. Kulish, H. J. Frenk and R. Kassing, Diamond and Related Materials, **1**, 164, 1992.
3. P. John, D. K. Milne and W. C. Vijayarajah, M. G. Jubber and J. I. B. Wilson, Diamond and Related Materials **3**, 388, 1994.
4. C. Wild, N. Herres and P. Koidl, Journal of Applied Physics **68**, 973, 1990.
5. C. Wild, P. Koidl, W. Muller-Sebert, H. Walcher, R. Kohl, N. Herrs and R. Locher, Diamond and Related Materials **2**, 158, 1993.
6. C. Wild, R. Kohl, N. Herrs, W. Muller-Serbert and P. Koidl, Diamond and Related Materials **3**, 373, 1994.
7. M. A. Tamor and M. P. Everson, Journal of Materials Research **9** (7), 1839, 1994.

III. Optical Properties of Epitaxial CeO_2 on Silicon Substrates

A. Introduction

Cerium oxide (CeO_2) is a rare-earth oxide which is non absorbing in the visible spectrum and has been used in optical coatings [1]. It has a face-centered cubic fluorite crystal structure that is closely matched to silicon [2] and recently there have been more research efforts to grow high quality CeO_2 single crystals on silicon substrates [3,4]. Potential applications of the insulating thin films are in high Tc superconductor structures, silicon on insulator (SOI) structures, and high-storage capacitor devices. The electrical characteristics of epitaxial CeO_2 films on silicon [4,5] and their use in high-storage capacitors were investigated. With optimized growth temperature and annealing time in oxygen at 900°C, device-quality MOS structures of CeO_2 films on silicon has been achieved [5]. The optical properties of CeO_2 were reported using spectral absorbance and reflectance measurements on glassy films and poly crystalline and bulk single crystal samples [6-8]. A sharp absorption band was consistently observed at about 3 eV and was attributed to transitions between the oxygen 2p band (valence band) and the cerium 4f band of CeO_2 which lies just above the Fermi level of the material [7]. This assignment was consistent with calculations of the electronic structure of CeO_2 [9] which indicated a band gap of about 5.5 eV separating the conduction band (Ce 5d band) and the valence band of the material with a 4f band (about 1 eV wide) lying 3 eV above the valence band.

This section reports further studies of the optical properties of single crystal CeO_2 films grown epitaxially on silicon and the effect of post annealing on the photoluminescence observed from the films. The photoluminescence observed from our high-quality single crystal films on silicon can give further information on the nature of optical transitions in CeO_2 and might open yet another application of the films in optical devices fabrication on silicon substrates.

B. Experimental Procedure

CeO_2 films were deposited on p-type Si(111) substrates using pulsed laser ablation following the procedure previously described in [3]. An ArF excimer laser was used to ablate a CeO2 target of 99.999% purity at a pressure lower than 10-7 Torr with the substrate temperature maintained at 650°C to deposit single crystal CeO_2. The film thickness was measured by ellipsometry and found to be about 1000 Å with an amorphous SiO_2 layer of about 40 Å formed at the silicon interface. The as-grown samples (sample A) were thermally treated by rapid thermal annealing in Ar at 1000°C for 5 minutes (sample B), and furnace annealing in O_2 at 1000°C for 6 hours followed by rapid thermal annealing in Ar at 1000°C for 5 minutes (sample C). Photoluminescence measurements were done using a He-Cd laser with a wavelength of 325 nm to excite electronic states in the samples.

C. Results

Figure 1 shows the *in situ* RHEED patterns obtained after deposition along the <110> and <11-2> directions of the substrate. The patterns indicate that the grown film was single crystal. X-ray diffraction rocking curve is shown in Fig. 2 showing a CeO_2 peak distinguished from the Si substrate diffraction peak of the (333) plane. The full width half maximum of the film peak was 45 arc sec indicating a very good quality of the crystal structure. The peak corresponds to a lattice constant of 5.4262 Å which is slightly larger than that of bulk CeO_2 of 5.4103 probably due to the strain in the grown CeO_2 films to match the silicon substrate and may also be due to the inclusion of oxygen vacancies in the films [10]. Figure 3(a-c) show the room temperature spectra obtained for samples A to C, respectively. The as-grown sample (A) showed a fairly broad spectrum as shown in Fig. 3(a). The other two samples exposed to rapid thermal annealing in argon, without O_2 annealing (sample B), and with 6 hours of O_2 annealing at 1000°C (sample C), showed a sharp emission peak in the violet/blue range with a FWHM of about 600 nm. The emission observed was stronger from thicker CeO_2 films.

D. Discussion

Previous studies of defects in CeO_2 crystals [10,11] showed that the fluorite crystal structure of the material remains intact over a relatively wide range of non-stoichiometric compositions through the inclusion of oxygen vacancies. The presence of these vacancies gives rise to an expansion of the lattice constant of the crystal as measured by x-ray diffraction. It is however very difficult to obtain an estimate of the oxygen deficiency of the films from x-ray data due to the lattice strain in the CeO_2 film to match the silicon substrate structure (about 0.35% at room temperature). Oxygen vacancies in CeO_2 crystals have energy levels in the band gap lower in energy than the 4f band states with temperature and concentration dependent occupancy. At low temperatures as was observed in electron paramagnetic resonance (EPR) studies done at liquid He temperature, electrons are trapped in oxygen vacancy sites rather than occupying 4f band states [12]. At higher temperatures, electrons are excited to the 4f band by electron-phonon interaction. Electrons so excited give rise to Ce^{3+} ions [11] where one of the two unoccupied 4f states of Ce^{4+} is occupied by an electron hopping between cation sites of the CeO_2 crystal. For large deviations from stoichiometry and larger vacancy concentrations the predominant charge state of vacancies is the singly ionized state where one level of the two levels of a vacancy is occupied. This gives rise to F+ centers in the crystal. For small deviations from stoichiometry and lower vacancy concentrations the dominant charge state of vacancies is the doubly charged state mainly to compensate for cation impurities of the material with lower valence. These give rise to F^{2+} centers [13].

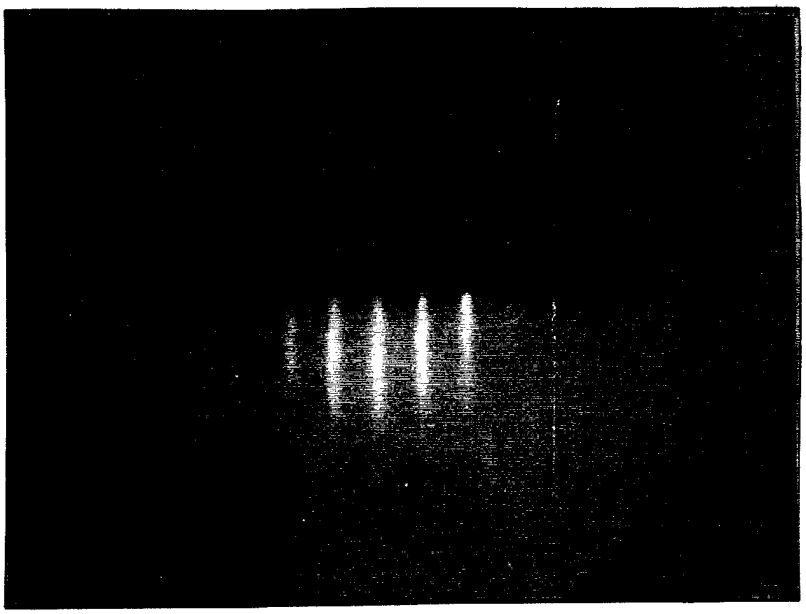

(a)

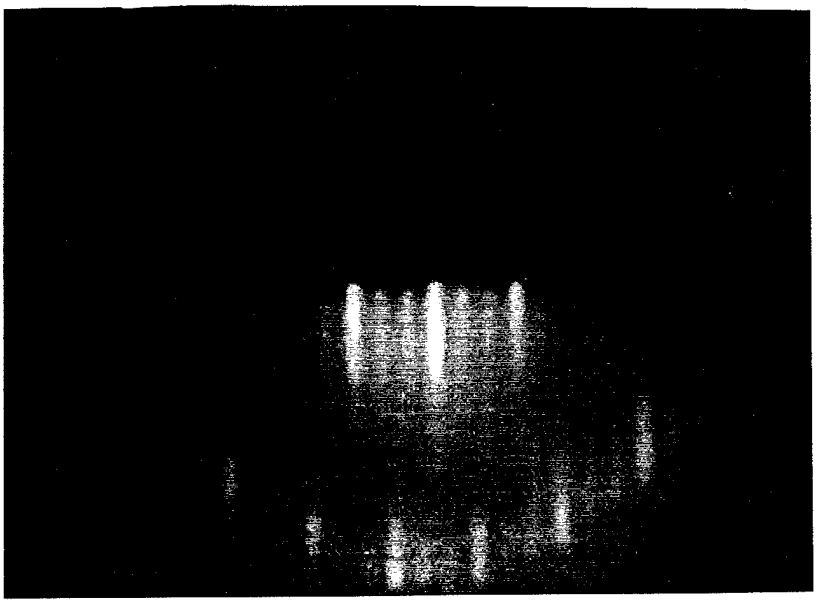

(b)

Figure 1. *In situ* Rheed patterns obtained after growth of CeO_2 on Si(111): (a) along the <110> and (b) the <11-2> directions of the substrate.

The broad photoluminescence of the as-grown films of Figs. 3(a) could be the result of defects including oxygen vacancies in the crystal with electronic energy levels lower in the band gap than the 4f band. These defects possibly act as radiative recombination centers for electrons initially excited from the valence band to the 4f band of CeO_2. An enhanced

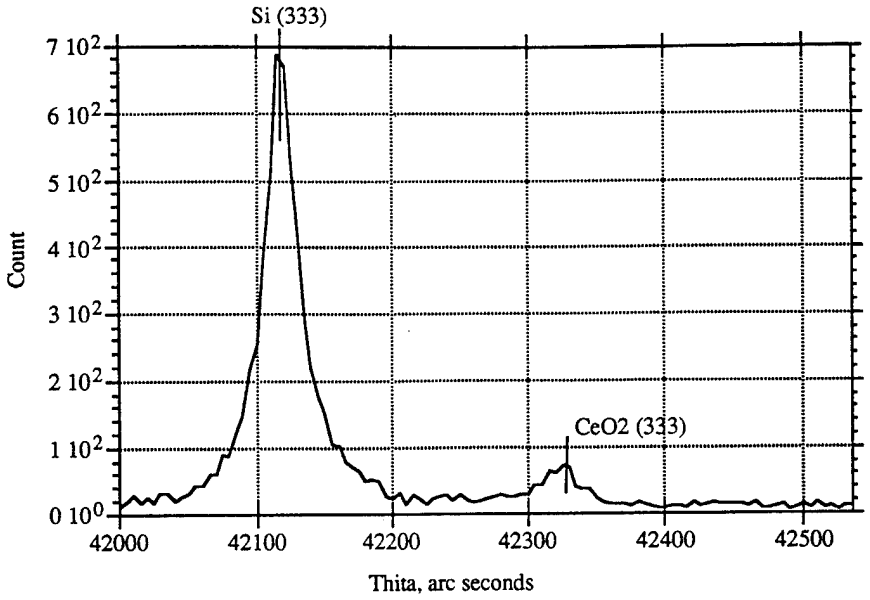

Figure 2. X-ray diffraction rocking curve of as-grown CeO_2 films deposited at 650°C.

absorption tail below 3 eV in non-stoichiometric CeO_2 was previously attributed to the presence of oxygen vacancies [8]. The effect of rapid thermal annealing on the photoluminescence can be explained by a curing of the crystal defects upon annealing. At high temperatures oxygen vacancies become relatively mobile where they can migrate to tie to lower valence impurities in the crystal or form vacancy aggregates. The effect of lowering the concentration of vacancies is to change their dominant charge state to doubly ionized where no electrons are there to undergo transitions to the valence band states available upon irradiation. These effects might explain the appearance of the 400 nm emission peak shown in Fig. 3(b) and (c) which coincides in energy with the 4f to valence band energy gap of 3.1 eV obtained from optical absorption measurements reported in the literature [6], and the diminishing of the broad photoluminescence observed from as grown samples. The effect was enhanced by the oxygen annealing of sample(C) at 1000°C for 6 hours before the rapid thermal annealing as compared to sample (B) where only rapid thermal annealing was done. The 400 nm emission peak was not observed from samples annealed in oxygen with no rapid thermal annealing cycles or from samples furnace annealed at 1000°C for 5 minutes in argon. The fact that reported optical absorption edge of CeO_2 films at 3.1 eV indicated non-direct transitions [6] does not rule out the possibility that emission across the 4f to 2p energy gap could be the origin of the luminescence detected after rapid thermal annealing of the samples. These transitions are charge transfer transitions and are thus electric-dipole allowed with a weak oscillator strength due to small electronic wave function overlaps [7]. They would give an emission at about 400 nm that is relatively sharp due to the nature of the 4f band of Ce in CeO_2 as outlined earlier.

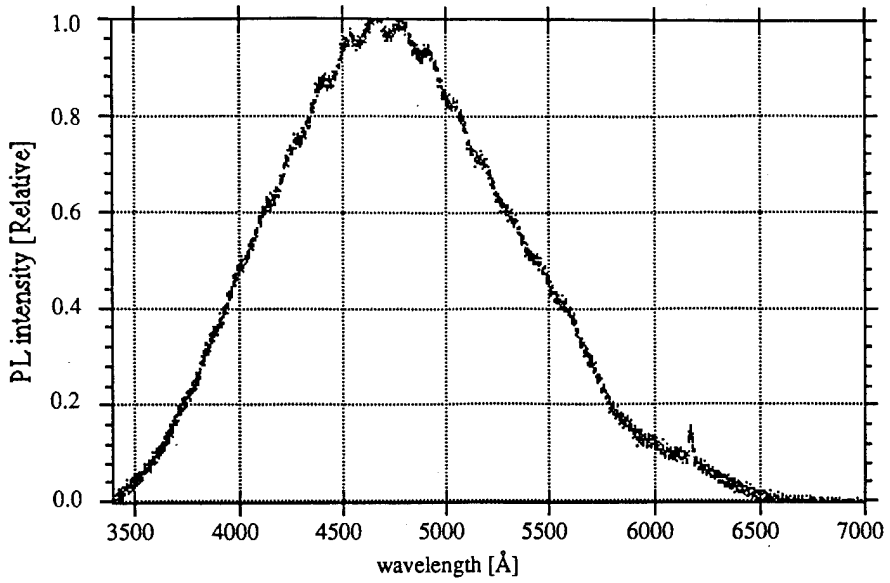

Figure 3(a). Room temperature photoluminescence spectrum of as deposited epitaxial CeO_2 films on Si(111);

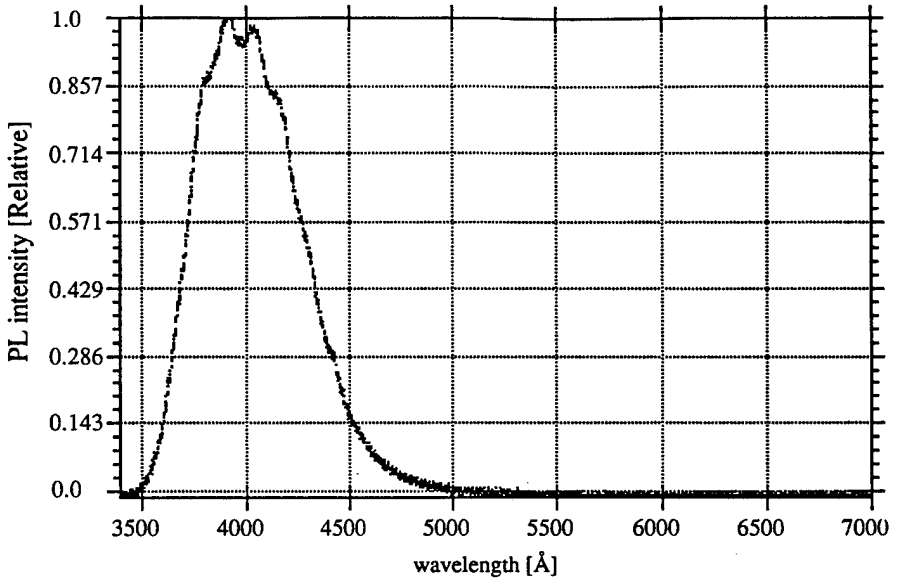

Figure 3(b). Room temperature photoluminescence spectrum of epitaxial CeO_2 films on Si(111) after 5 min. rapid thermal annealing in Ar at 1000°C;

E. Conclusions

In conclusion, we have reported on observing violet photoluminescence for the first time from annealed CeO_2 single crystal films grown by pulsed laser deposition of CeO_2 on silicon substrates and rapid thermally annealed in an argon environment at 1000°C. The single crystallinity of the films epitaxially deposited on Si(111) substrates was assured by the *in situ*

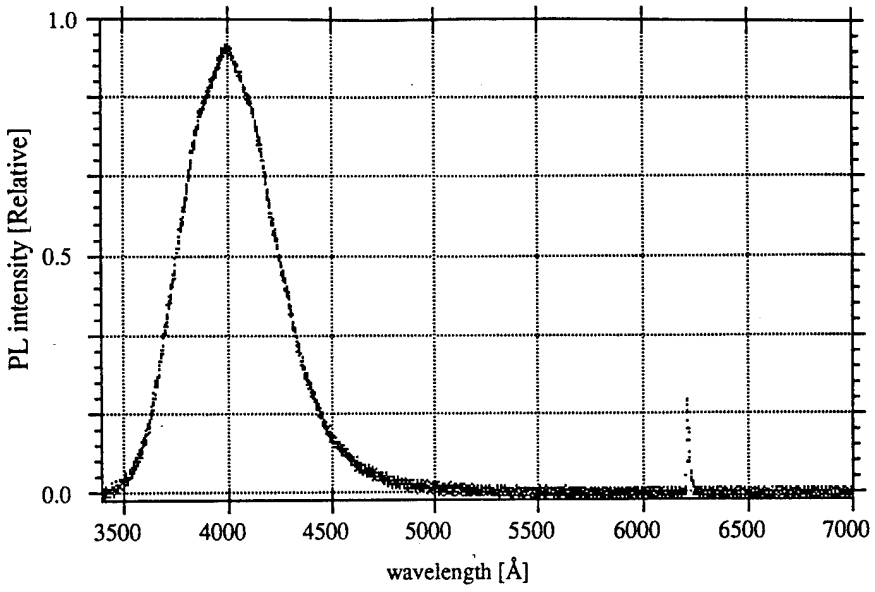

Figure 3(c). Photoluminescence spectra of epitaxial CeO_2 films on Si(111) after 6 hours annealing in O_2 at 1000°C followed by 5 min. rapid thermal annealing in Ar at 1000°C.

RHEED patterns and XRD rocking curves obtained. A strong photoluminescence emission at 400 nm was observed from thermally treated films upon excitation by a He-Cd UV laser. This emission can be due to charge transfer transitions from the 4f band to the valence band of CeO_2.

F. Future Research Plans and Goals

Further investigation of the origin of the reported emission and the possibility of its utilization to fabricate optical devices on silicon substrates are currently under further investigation.

G. References

1. G. Haas, J. B. Ramsey, and R. Thun, J. Opt. Soc. Am. **48**, 324, 1957.
2. *Gmelin Handbook der Anorganischen Chemie*, 8.Auflage, seltererdelemente 39, 230 (Springer, Berlin, Heiderberg, New York, 1974, in German)
3. T. Chikyow, S. M. Bedair, L. Tye, and N. A. El-Masry: Appl. Phys. Lett. **65**, 1030, 1994.
4. L. Tye, N. A. El-Masry, T. Chikyow, and S. M. Bedair: Appl. Phys. Lett. **65**, 308, 1994.
5. A. H. Morshed, M. Tomita, N. El-Masry, P. McLarty, N. P. Parikh and S. M. Bedair, *Proceedings of the Materials Research Society*, Fall 1995 Meeting, Boston MA, paper G3.9.
6. C. A. Hogarth and Z. T. Al-Dhhan, Phys. Status. Solidi B **137**, K157, 1986.
7. M. Niwano, S. Sato, T. Koide, T. Shidara, A. Fujimoro, H. Fukutani, S. Shin and M. Ishigama, J. Phys. Soc. Japan **57**, 1489, 1988.
8. F. Marabelli and P. Wachter, Phys. Rev. B **36**, 1238, 1987.

9. D. Koelling, A. Boring, and J. Wood, Solid State Comm. **47**, 227, 1983.
10. J. R. Sims, and R. N. Blumenthal, High Temp. Sc. **8**, 99, 111, and 121, 1976.
11. H. L. Tuller and A. Nowick, J. Phys. Chem. Solids **38**, 859, 1977.
12. I. Vinokurov, Z. Zonn and V. Ioffe, Sov. Phys. Solid State **9**, 2659, 1968.
13. B. Henderson, CRC Crit. Rev. Solid State and Mat. Sci. **9**, 1, 1980.

IV. Deposition of Crystalline Silicon on Lattice Matched CeO_2/Si(111) Substrates

A. Introduction

Cerium oxide is a promising material for the insulator in a SOI structure as it has a crystal structure which is closely matched to silicon. The lattice misfit factor for CeO_2 to silicon, $\Delta a/a = 0.35\%$, is better than the respective values for other crystalline insulators such as CaF_2, sapphire, and spinel. The SOI structure requires a thin single crystal layer of silicon of low defect density for the fabrication of electronic devices. These would be isolated by the insulator layer from the partially conducting silicon substrate [1]. High quality single crystal CeO_2 films have been grown and characterized as insulating oxide films on silicon [2, 3]. The same vacuum apparatus used for deposition of CeO_2 films on silicon by pulsed laser ablation was used to deposit silicon on CeO_2 *in situ* by injection of diluted 1% disilane in N_2 gas into the growth chamber. The growth mode of silicon on CeO_2 was probed by RHEED and optical microscope inspection of the films. Further investigation by high resolution transmission electron microscopy is undergoing.

B. Experimental Procedure

Single crystal CeO_2 films were grown by pulsed laser ablation of CeO_2 target under UHV conditions as previously described in [2] at 650°C. Diluted 1% disilane in N_2 gas was then injected into the growth chamber with on-line pumping at pressures of 1.5 and 3 mTorr with the substrate temperature kept at 700 and 750°C to grow silicon on CeO_2 by an LPCVD process [4]. Both (111) $\pm$ 0.5° and (111) 5° $\pm$ 0.5° off axis towards the <110> direction silicon substrates were used. The growth mode of silicon on CeO_2 was probed by RHEED and optical microscope inspection of the films.

C. Results

Figure 1 shows the RHEED pattern obtained after the deposition of silicon on CeO_2 grown on Si(111) substrate at a temperature of 700°C and a pressure of 1.5 mTorr for one hour. High resolution transmission electron microscopy indicated island growth of A- and B-type crystalline silicon on the CeO_2 film. Optical inspection indicated three-dimensional features on the surface. Growth at lower temperatures resulted in RHEED patterns similar to those of the CeO_2 films and no surface features. Increasing the growth temperature to 750°C resulted in the same RHEED patterns. We then increased the growth pressure to 3 mTorr and the runs duration to 2 hours and tried both (111) $\pm$ 0.5° and (111) 5° $\pm$ 0.5° off axis towards the <110> direction silicon substrates. Three dimensional features were then observed all over the samples with more density on tilted substrates. Figure 2 shows a photograph of the features observed on a tilted silicon substrate. Preparation of samples of these runs for HRTEM is ongoing.

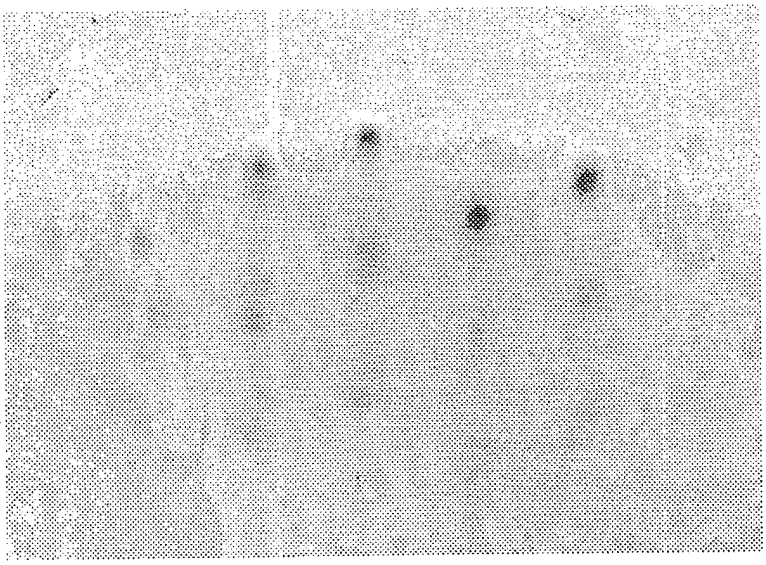

Figure 1. RHEED pattern along the <110> azimuth for silicon deposited on CeO_2 grown on Si(111) substrate at a temperature of 700°C and a pressure of 1.5 mTorr for one hour.

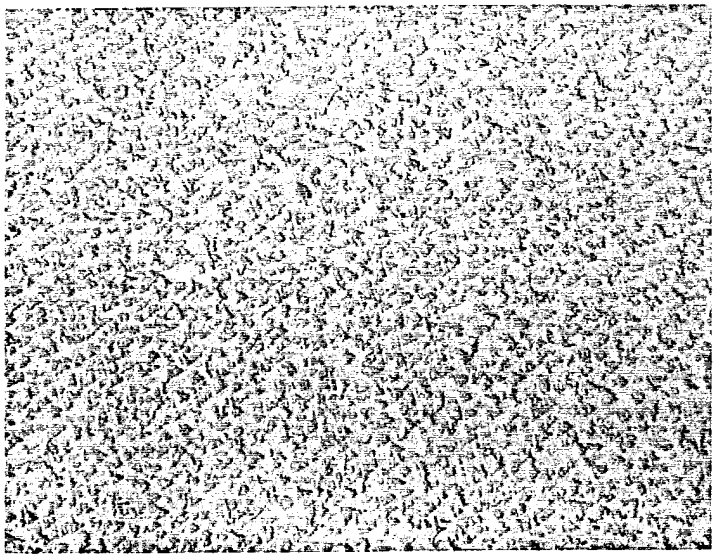

Figure 2. Optical microscope photograph of the surface of silicon deposited at 750°C and 3 mTorr for 2 hours on CeO_2 on a tilted silicon substrate.

D. Discussion

Both the RHEED patterns obtained and the optical microscope inspection of the films indicate a three-dimensional mode of growth of silicon on CeO_2 even on slightly off axis silicon substrates. A similar situation was reported for silicon grown on CaF_2 by MBE [5]. The RHEED patterns also indicate crystalline silicon deposition. However, the single

crystallinity of the films can not be confirmed. The grown films are too thin to be investigated for their crystallinity by x-ray diffraction.

E. Conclusions

Crystalline silicon was grown on nearly lattice matched CeO_2 on silicon (111) substrates by a LPCVD process. The growth mode of the films were found to be three dimensional by RHEED and optical microscope inspection.

F. Future Research Plans and Goals

The single crystallinity of grown silicon films is to be investigated by high resolution transmission electron microscopy. Control of the growth parameters to deposit single crystal silicon on CeO_2 in a two dimensional growth mode is planned.

G. References

1. J. C. Strum, Mat. Res. Soc. Symp. Proc. **107**, 295, 1988.
2. L. Tye, N. A. El-Masry, T. Chikyow, and S. M. Bedair: Appl. Phys. Lett. **65**, 308, 1994.
3. A. H. Morshed, M. Tomita, N. El-Masry, P. McLarty, N. P. Parikh and S. M. Bedair, *Proceedings of the Materials Research Society*, Fall 1995 Meeting, Boston MA, paper G3.9.
4. M. K. Sanganeria, K. E. Violette and M. Ozturk, Appl. Phys. Lett. **63**, 1225, 1993.
5. P.O. Petterson, R. J. Miles and T. C. McGill, Mat. Res. Soc. Symp. Proc. **367**, 305, 1995.

V. Distribution List

Mr. Max Yoder Office of Naval Research Electronics Division, Code 312 Ballston Tower One 800 N. Quincy Street Arlington, VA 22217-5660	3
Administrative Contracting Officer Office of Naval Research Regional Office Atlanta 101 Marietta Tower, Suite 2805 101 Marietta Street Atlanta, GA 30323-0008	1
Director, Naval Research Laboratory ATTN: Code 2627 Washington, DC 20375	1
Defense Technical Information Center Bldg. 5, Cameron Station Alexandria, VA 22314	2